JACS
JOURNAL OF THE AMERICAN CHEMICAL SOCIETY
Article
pubs.acs.org/JACS

# Electrodeposition of Isolated Platinum Atoms and Clusters on Bismuth—Characterization and Electrocatalysis

Min Zhou, Jeffrey E. Dick, and Allen J. Bard*

Center for Electrochemistry, Department of Chemistry, The University of Texas at Austin, Austin, Texas 78712, United States

Supporting Information

**ABSTRACT:** We describe a method for the electrodeposition of an isolated single Pt atom or small cluster, up to 9 atoms, on a bismuth ultramicroelectrode (UME). This deposition was immediately followed by electrochemical characterization via the hydrogen evolution reaction (HER) that occurs readily on the electrodeposited Pt but not on Bi. The observed voltammetric current plateau, even for a single atom, which behaves as an electrode, allows the estimation of deposit size. Pt was plated from solutions of femtomolar $PtCl_6^{2-}$, which allowed precise control of the arrival of ions and thus the plating rate on the Bi UME, to one ion every few seconds. This allowed the atom-by-atom fabrication of isolated platinum deposits, ranging from single atoms to 9-atom clusters. The limiting currents in voltammetry gave the size and number of atoms of the clusters. Given the stochasticity of the plating process, we show that the number of atoms plated over a given time (10 and 20 s) follows a Poisson distribution. Taking the potential at a certain current density as a measure of the relative rate of the HER, we found that the potential shifted positively as the size increased, with single atoms showing the largest overpotentials compared to bulk Pt.

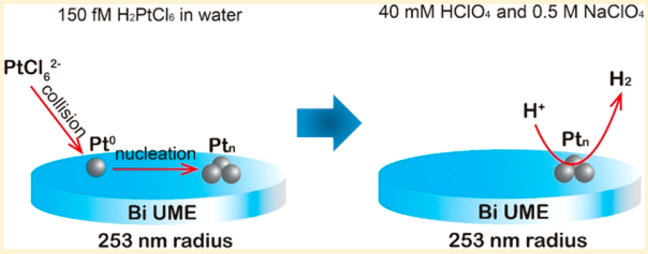


## INTRODUCTION

We describe a method for the electrodeposition of isolated single platinum atoms and small clusters by using very low concentrations of the plating precursor and hence limiting the diffusion rate of ions to the electrode. The size of the deposited Pt can be determined electrochemically by using the electrocatalytic amplification strategy.[1] Similarly, the relative rate of the electrocatalytic reaction can be determined, providing clear evidence of a size effect on reaction rate.[2]

To carry out this experiment a bismuth UME is first immersed in a fM $PtCl_6^{2-}$ solution, and a plating pulse of suitable duration is applied. The pulse duration dictates the number of platinum atoms plated on the UME assuming unit probability of $PtCl_6^{2-}$ reduction to $Pt^0$. The UME is then moved into a solution with a higher proton concentration. Bi shows a large HER overpotential, but the reaction occurs readily after platinum deposition, even at a single Pt atom. Steady-state voltammograms can be used to determine deposit size and relative reaction rate.

This approach has significant advantages over studies that use ensembles of nanoparticles (NPs), where polydispersity, aggregation, and capping agent effects can complicate analysis. One other significant advantage is that very small deposits can be fabricated and then characterized in solution. Earlier, we demonstrated a similar approach with larger (nm) Pt deposits on a carbon electrode.[3] Similar experiments to those described here were carried out with Pt on C fiber or pyrolyzed methane electrodes but suffered from problems in electrode stability and reproducibility.[4] On the basis of some preliminary experiments described here, we believe more detailed experiments can lead to new insights in mass transfer and electrochemistry at subnanometer electrodes and an understanding of nucleation and growth of metals at specific-active surface sites.

## RESULTS AND DISCUSSION

**Bismuth UME.** A Bi electrode was selected as the substrate for deposition because the HER is kinetically slow, and so the electrode shows a large overpotential for hydrogen evolution as shown in volcano plots[5] and the predicted correlation of reaction rate to melting point.[6] The preparation procedure of a Bi UME is given in the Supporting Information, Figure S1. Briefly, we first fabricated a cylindrical glass channel, filled it with Bi powder, melted it, and extruded the melted Bi liquid into the channel. After cooling, we mechanically polished the electrode and exposed a disk-shaped Bi UME. The disk radius was calculated from the steady-state voltammogram (Figure 1A) in a 5 mM methyl viologen ($MV^{2+}$) dichloride −0.2 M KCl solution. In the same solution, the voltammogram of 3.5 $\mu$m radius carbon UME showed a limiting current of 4.36 nA. On the basis of the ratio between the limiting currents, we calculated the radius of Bi UME as 253 nm. An SEM examination (Figure 1B) verified the size obtained from the electrochemical measurement.

The use of a small UME, as shown in nonclassical electrochemical nucleation and growth experiments with

Received: October 5, 2017
Published: November 13, 2017





DOI: 10.1021/jacs.7b10646
J. Am. Chem. Soc. 2017, 139, 17677−17682

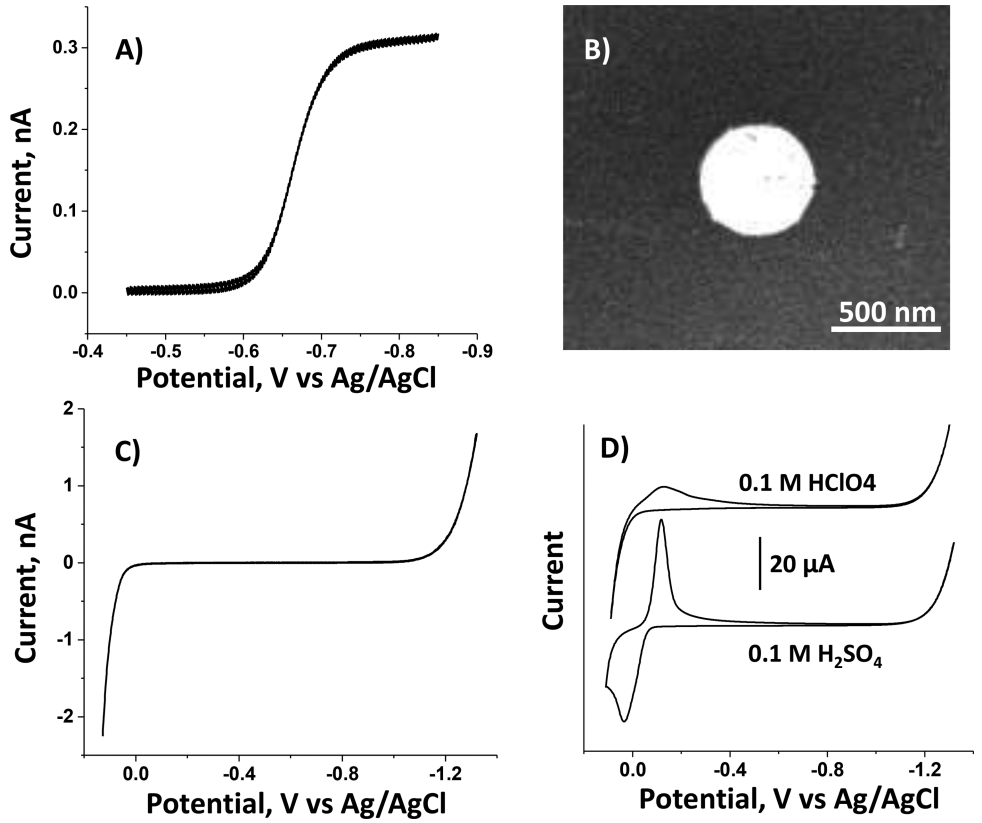


**Figure 1.** (A) Cyclic voltammogram of Bi UME in 5 mM $MVCl_2$ and 0.2 M KCl. (B) SEM image of Bi UME. (C) Cyclic voltammogram of Bi UME (253 nm radius) in 40 mM $HClO_4$ and 0.5 M $NaClO_4$ solution. (D) Cyclic voltammogram of Bi macroelectrode (0.5 mm radius) in 0.1 M $H_2SO_4$ and 0.1 M $HClO_4$ solutions. All scan rates were 0.1 V/s, and solutions were deaerated.

different metals, leads to only a single nucleus, rather than multiple deposits.[3] After polishing, microscopic examination (Figure 1B) showed that the surface of Bi UME was flat and smooth, with a mirror-like appearance. Figure 1C displays the potential window on a Bi UME (253 nm radius) in 40 mM $HClO_4$ and 0.5 M $NaClO_4$ solution (the solution was used for the latter HER studies), in which the cathodic and anodic sides were, respectively, controlled by the HER and Bi metal oxidation. Since Bi is easily oxidized (at 0 V vs Ag/AgCl), the redox mediator of $MVCl_2$ (with $E^0 = -0.25$ V vs Ag/AgCl) was selected in the former electrochemical characterization. Bi showed a similar negative range as C for the HER, as observed in Figure 1C. Moreover, the background current in the window did not show any impurity waves. Bi has a larger thermal expansion coefficient than borosilicate glass, so when the molten Bi metal hardens at the nanopore end of the capillary the sealing of Bi UME was tight, as seen by the flat background voltammetric curve, i.e., showing no leakage (Figure 1C). The extremely small background current (2 pA at 0.1 V/s) allowed a high sensitivity and signal/noise ratio in the amplification characterization experiment. To better understand Bi material, we also performed voltammograms of Bi macroelectrode (0.5 mm radius) in 0.1 M $H_2SO_4$ and 0.1 M $HClO_4$ solutions (Figure 1D). The anodic and cathodic behaviors of Bi were observed to be identical to the previous studies. Because of the really high mass-transfer rate of Bi UME (253 nm radius), a redeposition of Bi metal after oxidation did not occur in Figure 1C.

**Experimental Protocol.** As shown in Figure 2, the protocol consisted of electrochemical plating and detection

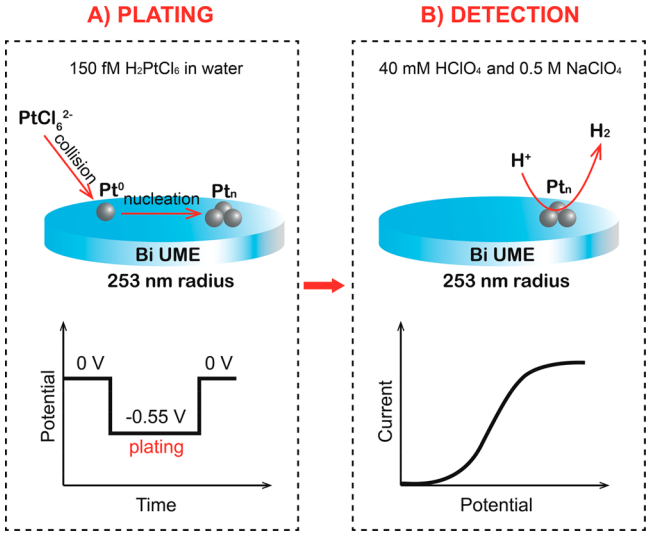


**Figure 2.** Schematic representation of the experimental protocol for a single platinum cluster deposition and subsequent detection by voltammetry of the HER.

steps. In the plating, we chose a 253 nm radius Bi UME and 150 fM $H_2PtCl_6$. A multiple potential step program was applied for controlled deposition, in which 0 and −0.55 V were biased to turn the plating off and on, respectively. To avoid the deactivation of the plated Pt, we prepared $H_2PtCl_6$ only in ultrapure water. In these cases, the deposition mechanism can be depicted as reduction of single impacting ions and subsequent nucleation and growth of single atomic clusters.[3]



DOI: 10.1021/jacs.7b10646
J. Am. Chem. Soc. 2017, 139, 17677−17682

When the adsorption interaction between the loaded atoms and the substrate is strong,[2] the plating efficiency could be close to 100%. Accordingly, the loading frequency ($f$) under the limiting diffusion control can be written as

$$f = 4DcaN_A \quad (1)$$

where $D$ is the diffusion coefficient of $PtCl_6^{2-}$ ($1.2 \times 10^{-5}$ cm$^2$/s), $c$ is the concentration (150 fM) of $H_2PtCl_6$, $N_A$ is Avogadro's number ($6.02 \times 10^{23}$ mol$^{-1}$), and $a$ is the radius (253 nm) of the Bi UME. In our case, the estimated frequency is about 0.1 Hz or one Pt atom deposited every 10 s.

**Characterization. Single Atoms.** After the plating, we detected the catalytic HER on the deposited Pt. The solution for the detection was 40 mM $HClO_4$ and 0.5 M $NaClO_4$. These concentrations of proton and electrolyte were appropriate for electrocatalytic amplification via the HER with no hydrogen bubble formation and with suppression of bulk migration of proton ions and diffuse-layer effect to the subnanometer Pt deposits. The single $Pt_1$ atom catalyst on the Bi substrate can produce a steady-state voltammogram of the HER (vide infra).

A key issue in characterization is the determination of the size, e.g. radius, of the deposit. In previous studies of NP (radii 5−200 nm) collisions, using the electrocatalytic amplification approach, the equation employed treated the catalyst as a nanosphere supported on an infinite flat substrate. The limiting diffusion current ($i_l$) to determine the radius ($r$) of the NP is[7]

$$i_l = nF[4\pi(\ln 2)]Dcr \quad (2)$$

based on treating the electrode as a sphere, where the terms in brackets represent a geometrical factor involving the area of the sphere partially blocked by the substrate. $F$ is the Faraday constant (96 485 C/mol). For proton reduction, $D$ is the diffusion coefficient ($9.3 \times 10^{-5}$ cm$^2$/s) and $c$ is the proton concentration (e.g., 40 mM).

However, for atoms or small clusters, representing the deposits as spheres is not appropriate, especially in trying to account for an exclusion zone. For this reason treatment of the deposit as a hemisphere, eq 3, seems more appropriate and is used throughout this paper.

$$i_l = nF[2\pi]Dcr \quad (3)$$

Here, $r$ is the equivalent radius of the deposit.

As shown below, the smallest $i_l$ value for atoms, i.e., $Pt_1$, yields an $r$ of 0.25 ± 0.05 nm, which is similar to accepted values of platinum radii.[8]

**Characterization. Multiatom Clusters.** Because of the stochastic nature of the deposition, multiple depositions for the same plating time will result in voltammograms with limiting currents of different heights, as shown in the Supporting Information, Figures S2 and S3, and discussed below. These can be grouped according to the limiting current and the half-wave potential within a small statistical variation (Table 1). We then assume that the voltammogram with the next higher limiting current represents a two-atom cluster, $Pt_2$, etc. A priory estimate of the "equivalent radius", $r_e$, is difficult since it depends on the cluster structure and the diffusion paths of protons to the clusters. What is given in Table 1 are experimental $r_e$ values assuming one can consider the cluster as a hemisphere with radius, $r$.

To obtain a rough value for the number of Pt atoms in a cluster from the limiting current (Figure 3A) we found them empirically and assume throughout proportionality with respect to area, i.e.

**Table 1. Single Pt Clusters Prepared from the Protocols of 10 and 20 s Plating**[a]

| $Pt_n$ | $i_l$ (pA) | $r$ (nm) | $E_{1/2}$ (V) | $E$ at $j$ = 12.6 pA/nm$^2$ (V) |
|---|---|---|---|---|
| $Pt_1$ | 56 (12) | 0.25 (0.05) | −0.57 (0.02) | −0.49 |
| $Pt_2$ | 91 (9) | 0.40 (0.04) | −0.54 (0.03) | −0.47 |
| $Pt_3$ | 109 (6) | 0.48 (0.03) | −0.51 (0.02) | −0.46 |
| $Pt_4$ | 121 | 0.54 | −0.48 | −0.44 |
| $Pt_5$ | 144 | 0.64 | −0.46 | −0.42 |
| $Pt_9$ | 169 | 0.75 | −0.44 | −0.40 |

[a]Note: The values in parentheses are standard deviations from the average value, and all potentials are vs NHE. $Pt_n$ ($n \leq 5$) are from the plating of 10 and 20 s. $Pt_9$ is uniquely prepared from the 100 s plating. The standard deviations for $Pt_1$, $Pt_2$, and $Pt_3$ are calculated from 11, 10, and 4 different trials. Others are single trials. The potential at 12.6 pA nm$^{-2}$ for bulk Pt (5 $\mu$m radius UME) is −0.23 V vs NHE.

$$i_l = nFAmc \quad (4)$$

where $m$ is the mass transfer rate constant to a single atom, i.e., $D/r_1$, where $D$ here is for proton and $r_1$ = 0.25 nm.

Assuming the atoms in the initial stages of nucleation and growth all conform to a close-packed arrangement on the Bi substrate surface (i.e., two-dimensional structure), one can estimate the number of atoms in a cluster by dividing the area of the cluster by the area of a single atom. Note this evaluation is probably more accurate when there are only a few atoms, e.g., 2 or 3, than larger clusters. If one takes the radius of a platinum atom as ca. 0.25 nm then $(0.40/0.25)^2 \cong 2$ atoms, $(0.48/0.25)^2 \cong 3$, $(0.54/0.25)^2 \cong 4$ atoms, and so on. The numerical estimate has to be combined with the Poisson statistics analysis (vide infra) to evaluate the number of atoms in a cluster. For instance, the value of $(0.40/0.25)^2 = 2.56$ is uncertain because it is not a unique integer. Nevertheless, by comparing our results with what is predicted using Poisson statistics, we could determine the value was most probably 2 and not 3.

Figure 3A shows representative voltammograms of deposits ranging from single platinum atoms up to clusters of 9 atoms. Figure 3B shows the current densities plotted as a function of potential. From the plot in Figure 3A, there is a clear positive shift in the half-wave potential as well as an increase in the steady state limiting current values as more platinum is deposited. The shift in potential indicates that the platinum atoms are forming a single growing nucleus on the Bi UME surface. If isolated platinum atoms were formed and well separated on the surface, one would expect an increase in limiting current with a single half-wave potential characteristic of $Pt_1$. Thus, this observation indicates a kinetic size effect of platinum clusters which should approach the bulk half-wave potential for polycrystalline platinum deposits. Figure 4A and 4B shows how the limiting current and the potential defined at a given current density, respectively, change as a function of the number of atoms deposited. Due to uncertain and complicated mechanisms of HER on Pt atomic deposits, we compared the relative rates of the HER at a given current density, 12.6 pA nm$^{-2}$, located in the kinetically controlled region (i.e., $i \ll i_{lim}$) of the voltammogram (Figure 3B). From the results in Figure 4B, we find that with an increase of the number of atoms in a cluster, the potential at the defined current density shifts in the positive direction, corresponding to a smaller overpotential (compared to bulk Pt) and higher HER reaction rate.

**Poisson Distributions.** The plating of single Pt atoms on a substrate is a stochastic process. Thus, for experimental trials



DOI: 10.1021/jacs.7b10646
J. Am. Chem. Soc. 2017, 139, 17677−17682

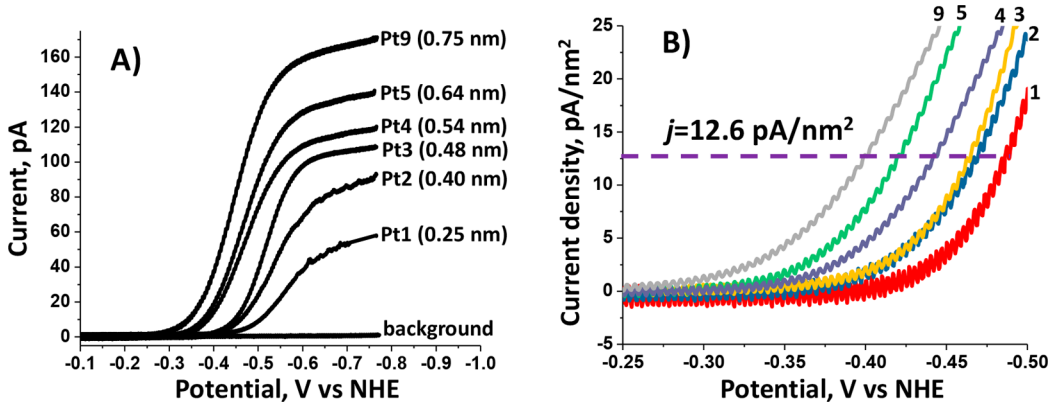


**Figure 3.** (A) Typical voltammograms of single Pt atoms and clusters in a deaerated 40 mM $HClO_4$ and 0.5 M $NaClO_4$ solution. Scan rate was 50 mV/s. Estimation of the size and atom number of the single clusters is discussed in the main text. For clarity, only forward scans are shown. Typical complete scans for reversal are shown in the Supporting Information. (B) Current density vs potential curves obtained from the forward segments of voltammograms in A, at a current density $j$ = 12.6 pA/nm$^2$, were used to evaluate the relative heterogeneous rates. Value was arbitrarily selected within the kinetic-limited region. Current density was calculated by dividing the current by the hemispherical area of single cluster (i.e., $2\pi r^2$). Labeled curves in B are consistent with those in A.

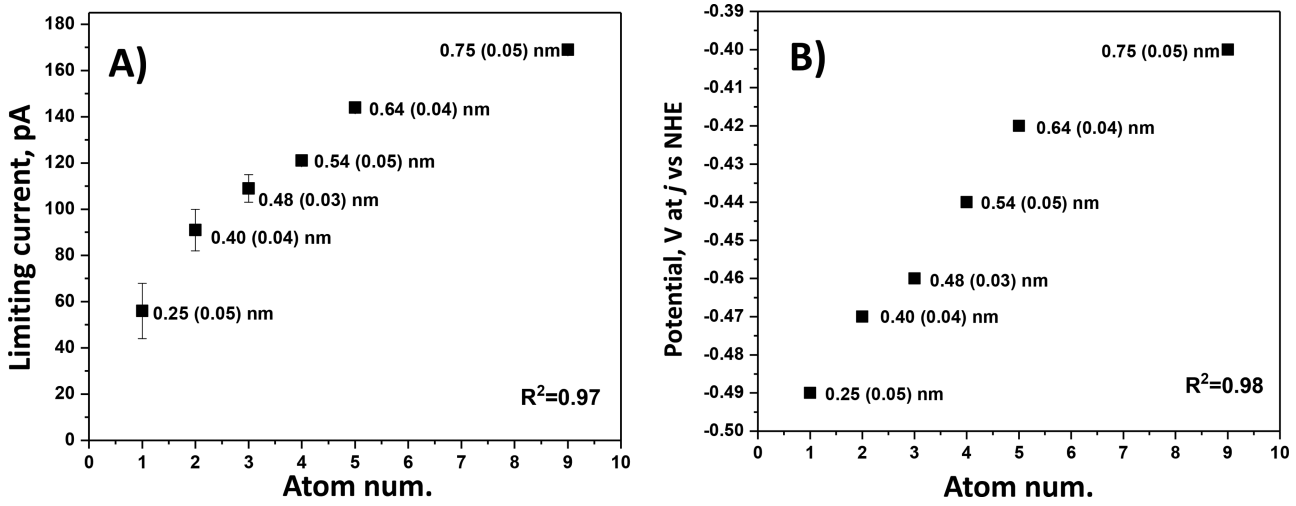


**Figure 4.** Limiting current and potential at the defined current density shown in Figure 3, respectively, correspond to the estimated atom number in a single cluster.

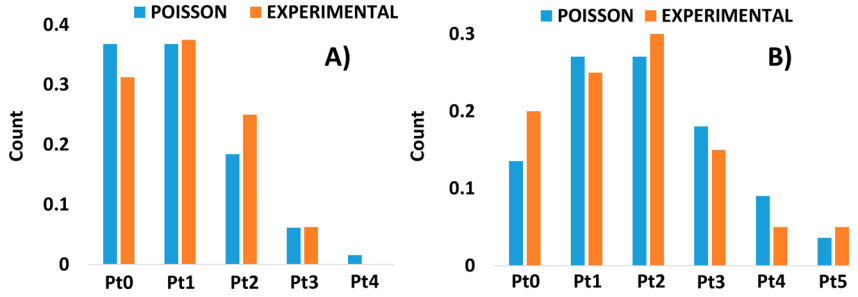


**Figure 5.** Histogram of the number of atoms calculated by the limiting current overlaid with a Poisson distribution when the deposition times were 10 (A) and 20 (B) s, respectively. These data include 16 and 20 total experiments, respectively.

involving an average time for deposition of 1 atom, statistically 0, 1, 2, 3, or 4 atoms can be deposited. The distribution of sizes is given by a Poisson probability distribution

$$P(k, \lambda) = \frac{\lambda^k e^{-\lambda}}{k!} \quad (5)$$

where $\lambda$ is the expected or most probable value (e.g., for 10 s deposition, $\lambda \cong 1$; for 20 s, $\lambda \cong 2$...) and $P(k, \lambda)$ is the probability of size $k$ where $\lambda$ is the expected value. Taking the 10 s plating as an example, the expected events of single atom deposition is $i$ = 1, while the other possible events during a single-atom plating experiment are $k$ = 0, 1, 2, 3, 4. The related probability is $P(0,1)$ = 37%, $P(1,1)$ = 37%, $P(2,1)$ = 18%, $P(3,1)$ = 6%, and $P(4,1)$ = 1%. Thus, $P(3,1)$ represents the probability of 3 single-atom deposition events occurring within 10 s. As noted above, the platinum deposits and nucleates at a



DOI: 10.1021/jacs.7b10646
J. Am. Chem. Soc. 2017, 139, 17677−17682

single site on the Bi UME surface, meaning 3 single atoms form a $Pt_3$ cluster. As a control experiment, we chose a deposition time where the average number of deposited atoms would be <1 atom and close to 0 (i.e., depositions for 3 s when the expected arrival rate to the electrode surface is one ion every 10 s). From the Poisson equation above, one would predict that deposition would be rare, i.e., at the limit of 0 (since $0^k$ is always 0). For 10 trials with deposition times of 3 s, no catalytic activity was detected after plating. In 16 trials with a deposition time of 10 s, limiting currents consistent with $Pt_0$, $Pt_1$, $Pt_2$, and $Pt_3$ were observed. Figure 5A presents a distribution of the number of Pt atoms calculated as described above, and this distribution is in good agreement with the computed Poisson distribution. Figure 5B also demonstrates a reasonable agreement between the Poisson distribution and the experiments (20 trials) for the 20 s plating. Longer deposition times are more difficult to compare since the predicted Poisson distribution broadens, and the probability of precise deposition of a certain number of atoms diminishes. This is evident by comparing the probability for 1 atom in Figure 5A and the probability for 2 atoms in Figure 5B (~37% accuracy compared to ~28% accuracy). The actual probability is also affected by the nucleation time in addition to the stochastic nature of ions arriving and reducing (assuming unit probability) to $Pt^0$.

**Nucleation and Growth of Clusters.** In this study, we did not perform experiments designed to investigate the nucleation of clusters and the process of their growth. However, this clearly must be different than the classical thermodynamic theory of nucleation as developed by Gibbs,[9] Volmer and Weber,[10] Becker and Doring,[11] Frenkel,[12] and Zeldovich[13] and later expanded to the nucleation of metals on an electrode surface by Fleischmann,[14] Sluyters,[15] and Scharifker.[16,17] In classical nucleation and growth theory, a critical nucleus size must be reached before the new phase spontaneously grows.[18] In the initial stages of nucleation and growth, a birth rate and death rate dictate the induction time[19] for this critical nucleus to form and then spontaneously grow. For electrodeposition, this model relies on the assumption that the surface on which the new phase is electrodeposited is uniform in nature.[20] Interestingly, the deposition of single atoms and clusters seems to defy this model, implying metastable atoms and clusters can exist on energy-favorable surface sites at the electrode surface. One can monitor the nucleation and growth of single nuclei by using micro- and nanoelectrodes.[21] The relatively small area of these electrodes lowers the probability that multiple nuclei will grow.[22] By biasing the electrode potential where the deposition is diffusion controlled, the growth of a nucleus can be monitored in the amperometric response as an increase with $t^{1/2}$.[23] To emphasize this point we carried out experiments monitoring the induction time for the formation of the critical cluster for larger particles and subsequent spontaneous growth for $PtCl_6^{2-}$ on carbon electrodes as a function of the concentration of $PtCl_6^{2-}$. The amperometric responses for these experiments are given in the Supporting Information, Figure S4. From a plot of the induction time as a function of concentration of $PtCl_6^{2-}$ (plotted in millimolar), an inverse relationship was observed. From this relationship ($y = 6.7x^{-1.07}$, $R^2 = 0.96$, where $y$ is the time and $x$ is the concentration), one would expect the induction time at the femtomolar level to be on the order of $3.3 \times 10^{11}$ s or ~10 000 years; however, in our studies, we are able to observe catalysis after seconds of deposition. One other implication of our model is that the atoms very rapidly sample a large portion of the electrode before finding the most energy-favorable site, perhaps analogous to the facilitated diffusion model proposed for target location in some biological systems.[24−26]

## CONCLUSION

Because of the inert nature of a Bi-UME substrate, we successfully electrodeposited isolated single-platinum atoms and clusters that we could observe against the Bi background using the electrocatalytic amplification scheme. We achieved this in two steps: We first used femtomolar concentrations of $PtCl_6^{2-}$ to control the mass transfer of precursor ions to the electrode surface and, therefore, limit the number of Pt atoms plated on the electrode. We then detected the deposited single Pt atoms or clusters by voltammetry of electrocatalytic HER. We found that even single Pt atoms could give well-defined steady-state voltammograms differentiated from the background. Few atom clusters ($\leq Pt_9$) were fabricated through an atom-by-atom basis, the growth of which was observed in an increase in limiting currents and a positive shift in the defined potential for proton reduction. The limiting current was used to calculate the size of the deposited atoms and clusters. A 2D packing model for the structures was assumed to calculate the number of atoms in the clusters grown ($\leq Pt_9$), which was consistent with the plating time. We show that deposition of femtomolar precursors can be described by stochastic Poisson statistics in which the occurring events matched well with the theoretical prediction. These results indicate that catalytic structures can be fabricated on an atom-by-atom basis and further evaluation of their catalytic activity rigorously carried out in situ directly after deposition.

## ASSOCIATED CONTENT

### Supporting Information

The Supporting Information is available free of charge on the ACS Publications website at DOI: 10.1021/jacs.7b10646.

Chemicals and materials; preparation of fM analytes; fabrication of Bi UME; electrochemical measurements; detection voltammograms of HER on Pt deposits; nucleation and growth of Pt clusters (PDF)

## AUTHOR INFORMATION


### Corresponding Author

*ajbard@cm.utexas.edu

### ORCID

Jeffrey E. Dick: 0000-0002-4538-9705

Allen J. Bard: 0000-0002-8517-0230


### Notes

The authors declare no competing financial interest.

## ACKNOWLEDGMENTS

We acknowledge support of this research from the National Science Foundation (CHE-1405248, A.J.B.; DGE-1110007, J.E.D.) and the Robert A. Welch Foundation (F-0021).

## REFERENCES


(1) (a) Xiao, X.; Bard, A. J. *J. Am. Chem. Soc.* **2007**, *129*, 9610. (b) Dick, J. E.; Bard, A. J. *J. Am. Chem. Soc.* **2015**, *137*, 13752.

(2) Zhu, C.; Fu, S.; Shi, Q.; Du, D.; Lin, Y. *Angew. Chem., Int. Ed.* **2017**, *56*, 13944.

(3) Ma, W.; Hu, K.; Chen, Q.; Zhou, M.; Mirkin, M. V.; Bard, A. J. *Nano Lett.* **2017**, *17*, 4354.




DOI: 10.1021/jacs.7b10646
J. Am. Chem. Soc. 2017, 139, 17677−17682

(4) Dick, J. E. Ph.D. Dissertation, The University of Texas at Austin, 2017.
(5) Quaino, P.; Juarez, F.; Santos, E.; Schmickler, W. *Beilstein J. Nanotechnol.* **2014**, *5*, 846.
(6) Leonard, K. C.; Bard, A. J. *J. Am. Chem. Soc.* **2013**, *135*, 15885.
(7) Bobbert, P. A.; Wind, M. M.; Vlieger, J. *Phys. A* **1987**, *141*, 58.
(8) http://periodictable.com/Elements/078/data.html.
(9) Gibbs, J. W. *Trans. Connect. Acad. Sci.* **1876**, *3*, 108.
(10) Volmer, M.; Weber, A. Z. *Physikal. Chem.* **1925**, *119*, 277.
(11) Becker, R.; Doring, W. *Ann. Phys.* **1935**, *416*, 719.
(12) Frenkel, J. *J. Chem. Phys.* **1939**, *7*, 538.
(13) Zeldovich, J. B. *Acta Physicochim. USSR* **1943**, *18*, 1.
(14) Fleischmann, M.; Liler, M. *Trans. Faraday Soc.* **1958**, *54*, 1370.
(15) Milchev, A.; Kruijt, W. S.; Sluyters-Rehbach, M.; Sluyters, J. H. *J. Electroanal. Chem.* **1993**, *362*, 21.
(16) Scharifker, B.; Hills, G. *Electrochim. Acta* **1983**, *28*, 879.
(17) Gunawardena, G.; Hills, G.; Montenegro, I.; Scharifker, B. *J. Electroanal. Chem. Interfacial Electrochem.* **1982**, *138*, 225.
(18) Bindra, P.; Fleischmann, M.; Oldfield, J. W.; Singleton, D. *Faraday Discuss. Chem. Soc.* **1973**, *56*, 180.
(19) Sousa, J. P.; Pons, S.; Fleischmann, M. *J. Chem. Soc., Faraday Trans.* **1994**, *90*, 1923.
(20) Budevski, E. B.; Staikov, G. T.; Lorenz, W. J. *Electrochemical Phase Formation and Growth: An Introduction to the Initial Stages of Metal Deposition*; Wiley, 2008.
(21) Velmurugan, J.; Noel, J. − M.; Nogala, W.; Mirkin, M. V. *Chem. Sci.* **2012**, *3*, 3307.
(22) Abyaneh, M. Y.; Fleischmann, M.; Del Giudice, E.; Vitiello, G. *Electrochim. Acta* **2009**, *54*, 879.
(23) Abyaneh, M. Y.; Fleischmann, M. *J. Electroanal. Chem.* **2002**, *530*, 89.
(24) Halford, S. E.; Marko, J. F. *Nucleic Acid Res.* **2004**, *32*, 3040.
(25) Von Hipel, P. H.; Berg, O. G. *J. Biol. Chem.* **1989**, *264*, 675.
(26) Hu, T.; Grosberg, A. Y.; Shklovskii, B. I. *Biophys. J.* **2006**, *90*, 2731.


DOI: 10.1021/jacs.7b10646
*J. Am. Chem. Soc.* 2017, 139, 17677−17682